Performance and Exhaust Emissions of a Spark Ignition Internal Combustion Engine Fed with Butanol–Glycerol Blend

Stanislaw Szwaja [1,*], Michal Gruca [1], Michal Pyrc [1] and Romualdas Juknelevičius [2]

1 Department of Thermal Machinery, Faculty of Mechanical Engineering and Computer Science, Czestochowa University of Technology, Dabrowskiego 69, 42-200 Czestochowa, Poland; gruca@imc.pcz.pl (M.G.); pyrc@imc.pcz.pl (M.P.)

2 Faculty of Mechanics, Vilnius Gediminas Technical University, J. Basanavičiaus g. 28, LT-03224 Vilnius, Lithuania; romualdas.juknelevicius@vilniustech.lt

* Correspondence: szwaja@imc.pcz.pl; Tel.: +48-885-840-483

Abstract: Investigation of a new type of fuel for the internal combustion engine, which can be successfully used in both the power generation and the automotive industries, is presented in this article. The proposed fuel is a blend of 75% n-butanol and 25% glycerol. The engine tests conducted with this glycerol–butanol blend were focused on the performance, combustion thermodynamics, and exhaust emissions of a spark-ignition engine. A comparative analysis was performed to find potential similarities and differences in the engine fueled with gasoline 95 and the proposed glycerol–butanol blend. As measured, CO exhaust emissions increased, NOx emissions decreased, and UHC emissions were unchanged for the glycerol–butanol blend when compared to the test with sole gasoline. As regards the engine performance and combustion progress, no significant differences were observed. Exhaust temperature remarkably decreased by 3.4%, which contributed to an increase in the indicated mean effective pressure by approximately 4% compared to gasoline 95. To summarize, the proposed glycerol–butanol blend can be directly used as a replacement for gasoline in internal combustion spark-ignition engines.

Keywords: glycerol; butanol; gasoline; internal combustion engine; comparative analysis

1. Introduction

A by-product of the biodiesel production process is glycerol, which is quite widely used in the pharmaceutical and cosmetic industries [1]. Several studies have been conducted to adapt glycerol to the bio-refinery industry. It is well-known that glycerol is a by-product of the production of biodiesel from vegetable oil, mainly rapeseed oil [2]. To increase the production of biodiesel from renewable sources, an excess of glycerol production has been observed, which is difficult to neutralize. In this way, excess glycerol is considered a waste, posing a problem for biofuel producers. Presciutti et al. [3] found in their study that due to its low calorific value (LHV), its combustion is not an efficient way to produce energy. Therefore, the power generation industry is not interested in the use of glycerol as a fuel. The study conducted by Presciutti et al. disclosed that the combustion of glycerol with oxygen does not produce acrolein. The author also reviewed the prospects for the use of glycerol. On the contrary to the opinion by Presciutti, other researchers [4,5] shared the view that glycerol has a great potential as a fuel for thermal machines (IC motors, gas turbines, power boilers).

1.1. Glycerol Specific Properties

The main by-product of the production of biodiesel from vegetable oil is glycerol. It is reported that approximately 4200 megaliters of crude glycerol were extracted worldwide in 2020 [6]. Recently, the price of glycerol has dropped by about 6 times. Since the annual production of glycerol increased twice from 2001 to 2011, the price of crude glyceride

dropped from ~500 \$/t to ~100 \$/t during the same period. This tendency was the result of a biodiesel production increase from 0.2 mln. t to 9 mln. t within the period 2001–2012. The price of crude glycerin today remains at 44–70 \$/t because it was dumped with a fast increase in biodiesel production [5]. Thus, its use in the power supply industry has become economically viable. Glycerol has a relatively low calorific value. It is very viscous, so its injection in an internal combustion engine causes difficulties. It has a relatively high auto-ignition temperature of almost 643 K.

The physical properties of glycerol are given in Table 1 [7,8].

Table 1. Glycerol's main physical properties [5,6].

Property	Unit	Number
Water content	%	14–17
Mineral content (mainly alkaline)	%	6–8
Other organic compounds	%	<5
Methanol content	%	<1
Kinematic viscosity at 25 °C	m^2/s	$(450–750) \times 10^{-6}$
Characteristics of the combustion reaction at stoic. ratio in air		
Heat of combustion	MJ/kg	18
	kJ/mol	1662
Lower heating value (LHV)	MJ/kg	16
Gibbs free energy	kJ/mol	−2211 [1]

[1]—from our own calculations.

A series of experiments has been performed investigating the combustion of glycerol in a boiler burner [3,9–11]. To increase the combustion temperature of glycerol and its complete burning, Presciutti et al. [3] proposed co-combustion of glycerol with oxygen. Zhu [12] studied the co-combustion of glycerol with biochar and defined that the involvement of glycerol in the combustion process significantly shortens the combustion delay and increases the combustion rate of glycerol droplets. Bohon and Roberts [9] conducted studies in which fossil fuel was replaced by crude glycerin in combined heat and power plants. Studies have shown that crude glycerol contains a large amount of chemically bound oxygen, which can lead to significant reductions in NOx emissions. They suggested that the replacement of natural gas with crude glycerin could be done considering the price of conventional fuel and active stimulation of the market. Coronado et al. [10] investigated the ecological indicators of glycerol combustion in industrial boilers. They found that glycerol is a more environmentally friendly fuel and may therefore be a suitable alternative to diesel fuel, natural gas, and liquefied petroleum gas. Queiros et al. [11] conducted crude glycerol combustion tests with natural gas and hydrogen. They performed the tests under unreacted conditions in a laboratory furnace, spraying glycerol with two typical air-assisted atomizers. Their test results disclosed that the spray generated by these atomizers improves when the mass ratio of spray air to glycerol reaches 1. CO and HC emissions then decrease, and when this ratio increases to 1.5, NOx emissions increase. Significantly, the toxic component acrolein was not detected in their tests. Gupta and Kumar [6] concluded that the formation of acrolein, a harmful combustion product of glycerol, can be significantly reduced by burning glycerol at high temperatures. In summary, Gupta and other researchers argued that the burning of crude glycerol is not a suitable technology for glycerol utilization. The main reasons for this are the low boiling point, high auto-ignition temperature, formation of acrolein, and high salt content [6,10,13]. The high exhaust toxic emissions from glycerol combustion are a challenge that prompted scientists to develop an efficient combustion technology that could be implemented in heat and power generation machines. The large amounts of pollutants emitted during the combustion of glycerol and the reasons for their formation were studied by Rodrigues et al. [14]. According to their point of view, the crude glycerol needs to be purified in all cases, except in cases where direct combustion is used.

1.2. Glycerol Combustion in the Compression Ignition Engine

Researchers have identified several significant problems in attempting to apply glycerol in compression-ignition engines. A study performed by Grab-Rogalinski [15] presents that glycerol is difficult to burn at an ambient temperature due to its high viscosity. Therefore, Oprescu [16] proposed to process glycerol and burn the products obtained from its processing as additives to mixtures with fossil fuels. Eaton et al. [17] investigated the combustion of glycerol in a compression-ignition engine. In the tests, they used a mixture of diesel and glycerol, in which glycerol ranged from 10% to 20%. There was a problem with the stability of the mixture during mixing, so ultrasonic mixing was used to obtain a glycerol–diesel stable emulsion. The test revealed that the use of a mixture of diesel fuel and glycerol reduced emissions of nitrogen oxides (NOx) and particulate matter (PM) by 5–15% and 25–50%, respectively. Because the energy density of the glycerol–diesel emulsion is lower than that of pure diesel fuel, the indicative fuel consumption increased with increasing glycerol content in the emulsion. In the following study, Eaton et al. [17] also studied a 23% emulsion of glycerol and biodiesel. This emulsion was used as a fuel for a 1 MW, six-cylinder, medium-speed compression-ignition engine. Their study aimed to determine the effects of glycerol and biodiesel emulsion on combustion dynamics, emissions, and overall suitability. They stated that emulsion of glycerol and biodiesel reduced the carbon dioxide emissions during combustion despite a reduction in engine power. Considering that neither design nor technical modifications are required to the engine, such fuel may be suitable for power plants. Beatrice et al. [13] investigated the combustion of glycerol ether in an automotive compression-ignition engine. Tests have shown that glycerol derivatives present as additives in diesel fuel reduce the flashpoint of the mixture. Diesel blends with 10% and 20% by volume glycerol ether were tested. Beatrice found that glycerol ether has the biggest influence on the combustion process in the engine at low engine load due to the low cetane number (CN). Glycerol ethers are effective in reducing particulate matter (PM) emissions. At the end of the article, Beatrice recommended further research to evaluate the effectiveness of glycerol ether additives to control exhaust emissions. He also put forward the idea of adopting two independently operating injectors. One of them would inject an initial dose of diesel fuel that would initiate the ignition of the ethanol-glycerol mixture injected later. Gruca et al. [18] tested the combustion of a glycerol and ethanol mixture in a compression ignition engine at a ratio of 1:1 (50/50%). The tests showed that the NOx, UHC, and CO emissions did not change significantly when compared to the exhaust emissions of a diesel engine. Gruca also observed that the increase of glycerol–ethanol mixture in the total fuel injected into the engine cylinder significantly reduced the opacity. He found that with an increased amount of glycerol–ethanol fraction in the blend with diesel fuel, the opacity was reduced from 40 to 3 mg per cycle. This decrease is thought to be due to the oxygen content of the glycerol–ethanol mixture. Chwist et al. [19] and Grab-Rogalinski et al. [15] conducted several studies with two injectors. Both studies confirmed that the technology of direct injection enables the injection and combustion of a substantial amount of glycerol. In this way, one injector can be used to inject an initial diesel fuel pilot dose to initiate combustion and ignite the glycerol injected by the second injector.

1.3. Glycerol Combustion in the Spark-Ignition Engine

Glycerol, which is a cheap by-product extracted during the production of biodiesel, is also an attractive additive to either ethanol or butanol and can be used in a spark-ignition engine as a gasoline partial replacement. As Larsson et al. [9] investigated, oxygenated biofuels as alcohols and MTBE can successfully supplement gasoline for the spark-ignition engine. Apart from ethanol, n-butanol is currently under deep investigation to be applied as the fuel for spark-ignition engines [20,21]. According to studies by Quispe [5], which assessed economic aspects, it can be concluded that the use of glycerol in combination with alcohols (e.g., methanol, ethanol, butanol) may be economically viable. Hence, the strategy of mixing glycerol with n-butanol, as proposed in this paper, is justified from

both economic and technical points of view. However, a review of the literature shows that studies on glycerol combustion in spark-ignition engines are limited. The current research on glycerol combustion in reciprocating engines is mainly concerned with the use of a small amount of glycerol (up to a few percentage points by volume) that is blended with other fuels [13,17,22,23]. Such a mixture can be injected into the intake manifold (external mixture formation) or directly into the cylinder (internal mixture formation). Munsin and his group [23] conducted studies on the use of small amounts (up to 5%) of glycerol in the glycerol–ethanol mixture for a spark-ignition engine. He found that a small amount of glycerol improves the ignition process and reduces the injection rate by about 10% compared to combustion tests with pure ethanol. Stelmasiak and Pietras [24] tested a 10% blend of glycerol and methanol, which increased the overall engine efficiency by 2.0–7.8% compared to pure gasoline. It is quite widely known that ethanol is managed as the most commonly used gasoline fuel additive [25,26]. Ethanol blended with glycerol has a relatively high octane number, making it a viable fuel for spark-ignition engines.

A review of the studies shows that there are certain gaps in the area of combustion of butanol blended with glycerol in the spark-ignition engine. This article focuses on filling these gaps and providing knowledge in this field. The research work and the results presented in this article can be reasonably considered a new and innovative issue, which can characterize itself with big potential for implementation in the future, fulfilling demands from both the automotive industry and ordinary customers. The article discusses a method and describes a study on the efficient combustion of a hardly flammable liquid—glycerol, which is mixed with n-butanol in this case.

The main targets of this research to be realized are as follows:

- Combustion tests on a mixture of glycerol and n-butanol in an internal combustion spark-ignition piston engine,
- Emission tests on this engine,
- A recommendation to use the glycerol–butanol blend (Glyc_But) at a mixing ratio of 1:3, as a complete and suitable substitute for the gasoline 95 in a modern spark-ignition engine.

2. Materials and Methods

The methodology for the investigation proposed in the article is mainly concentrated on the following:

- To obtain knowledge on possibilities of glycerol combustion in a spark-ignited reciprocating engine. As glycerol characterizes itself with relatively high viscosity, butanol was proposed to dilute it and decrease its kinematic viscosity in this way to a level at which the blend can be successfully sprayed by a typical port-fueled gasoline injector.
- To obtain knowledge on toxic emissions from the engine fueled glycerol–butanol blend. Hence, the tests were focused on exhaust gas toxic emissions as follows: NOx, CO, UHC, and smoke.

The fuels applied for the research work were as follows:

- n-butanol–glycerol blend at the ratio of 3:1. Hence, the blend contains n-butanol at a percentage of 75%, whereas glycerol is present at 25% by volume. Purity of glycerol used for tests was 99.5% in weight. The glycerol–butanol ratio was selected regarding its viscosity, which should provide conditions for spraying and vaporization. Finally, the dynamic viscosity of this blend was in the range 0.9–1.4 mPas at 50 °C.
- Pure n-butanol 99.9%.
- Gasoline 95. This is characterized with an octane rating of 95 and is commonly used in the European market.

The n-butanol–glycerol blend was denoted in this article as Glyc_But. The physical properties of these fuels important for further analysis are presented in Table 2.

Table 2. Fuel applied for the research work and its physical properties [7,8,21,27,28].

Parameter	Unit	Gasoline 95 [28]	n-Butanol [21,27]	Glycerol [7,8]	Glyc_But [1]
LHV	MJ/kg	43.4	33.1	16.9	29.2
Density at NTP	kg/dm^3	0.735	0.810	1.252	0.923
Purity (Composition)	-	100%	99.9% wt	99.5% wt	25/75% vol
Air to fuel (A/F) stoichiometric ratio	-	14.97	11.15	5.20	9.13
Latent heat of evaporation	kJ/kg	350	582	974	715

[1]—from our own calculations.

Butanol and gasoline were used as reference fuels to provide comparative analysis and show differences and common features between these fuels and Glyc_But. At first, the investigation was focused on determining the optimal spark timing to obtain the maximum indicated mean effective pressure (IMEP). Next, progress in combustion expressed by combustion phases was under research. To provide the same initial conditions for the start of combustion, the spark timing was fixed for these tests. Finally, exhaust emissions tests were conducted under maximum engine load (maximum IMEP). A detailed description is presented in the section Test Matrix.

2.1. Test Matrix

The experimental work was divided into the three following main tasks:

- Investigation of optimal spark timing to obtain maximum brake torque (MBT) and maximum indicated mean effective pressure (IMEP). Additionally, the coefficient of variation (COV) of IMEP was introduced to express the smoothness of engine run.
- Combustion duration. Combustion analysis was carried out for the optimal spark timing. Two combustion phases were introduced as follows:
  - Initial combustion phase CA0-10
  - Main combustion phase CA10-90
- Toxic exhaust gas emission: NOx, CO, and UHC.

The combustion phase denoted CA0-10 characterizes the first stage of combustion starting from ignition until 10% heat is released. This is measured in crank angle (CA) deg. The CA0-10 is usually treated as the ignition delay. Next, combustion phase CA10-90 expresses crank angle for the remaining 80% of heat released during fuel combustion.

Detailed information on combustion tests conducted under this investigation is contained in Table 3. Firstly, preliminary tests were conducted to determine optimal spark timing corresponding to maximum engine power for each fuel. Next, combustion tests were realized at optimal spark timing and maximum power to obtain knowledge on combustion phases and exhaust toxic emissions.

Table 3. Test matrix.

Test No.	Fuels	Parameters	Value
Test 1 Preliminary investigation	Glyc_But n-Butanol Gasoline 95	Spark advance angle	(−2)–(−20)
		Relative equivalence ratio "lambda"	1.00–1.05
		Engine load	Maximum at WOT

Table 3. *Cont.*

Test No.	Fuels	Parameters	Value
Test 2 Combustion progress CA0-10 CA10-90	Glyc_But n-Butanol Gasoline 95	Spark advance angle	Optimal to obtain max. IMEP
		Relative equivalence ratio "lambda"	1.00–1.05
		Engine load	Max. IMEP
Test 3 Exhaust emissions at max. IMEP	Glyc_But n-Butanol Gasoline 95	Spark advance angle	(a) Varying (b) Optimal for max. IMEP
		Relative equivalence ratio "lambda"	1.00–1.05
		Engine load	Maximum at WOT

2.2. Test Setup

Figure 1 presents a diagram of the test bench used for research work. The main part of the test bench is the UIT 85 engine. It is a single-cylinder spark-ignited engine with a variable compression ratio that has had several modifications to work on various alternative fuels. The most important change was the modification of the fueling system. Nowadays, the engine is equipped with two systems: port-fueled injection and in-cylinder direct injection.
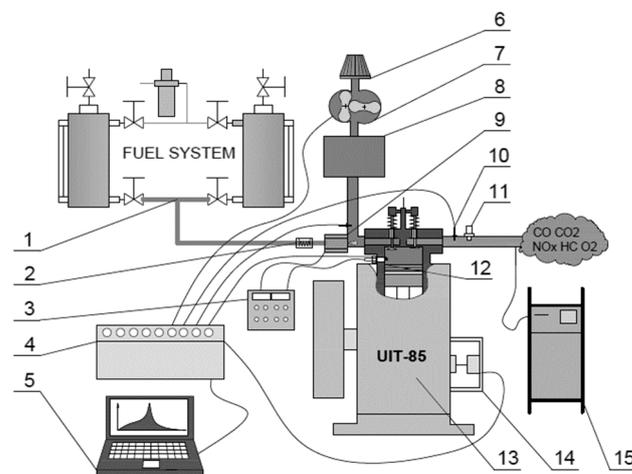

Figure 1. Test bench. 1—Refueling system; 2—Injector; 3—Electronic engine control system; 4,5—Data acquisition system with computer system; 6—Air filter; 7—Air flowmeter; 8—Surge tank of 120 dm^3 for suppressing pressure oscillations; 9—Air–fuel mixer; 10—Temperature sensor for exhaust gases; 11—Universal exhaust gas oxygen (UEGO) sensor; 12—Spark plug combined with a pressure sensor; 13—UIT-85 research engine; 14—Encoder; 15—Exhaust gas analyzing system.

The UIT-85 engine (13) is a research engine with a variable compression ratio in the range from 7 to 13.5. The engine was equipped with a fueling system (1) and PFI injector (2), a control system (3), and a data acquisition system (4,5). The injection pressure of the fuel system is set to 4 bar in the refueling tanks. The system uses an encoder (14) built on the camshaft for generating pulses that synchronize the in-cylinder pressure (12) with the engine crankshaft current positions. The measured parameters are analyzed in real-time conditions with the aid of a data acquisition system that collects data with a sampling frequency of 150 kHz. The airflow goes through the air filter (6) and the mixing unit (9) to the engine (13), and was measured by a rotor flow meter (7). A tank (8) with a capacity of 120 dm^3 was used to dump the pressure pulsations generated by the engine intake

port during the charge exchange process. The temperature sensor (10) and the wide-band UEGO sensor (11) are for measuring temperature and oxygen content in the exhaust gases, respectively. The Bosch gas analyzer (15) was used to measure toxic content in exhaust gases as follows: unburnt hydrocarbons (UHC), nitric oxides (NOx), and carbon monoxide (CO). The engine (13) worked at a constant speed of 600 rpm following conditions for octane rating measurements in the CFR engine. The load generated by the engine was dissipated in a brake unit consisting of a 3-phase asynchronous electric motor. Motor speed, as well as engine speed, were controlled by a frequency inverter of max. 5 kW brake power. Engine technical data is included in Table 4.

Table 4. Specifications of the engine UIT-85.

Type of Engine	Single Cylinder, Four-Stroke, Freely Aspirated
Ignition system	Spark ignited
Cylinder bore	85 mm
Piston stroke	115 mm
Connecting rod length	266 mm
Swept volume	652 cm^3
Compression ratio	9.5:1
Crank shaft speed	600 rpm

2.3. Error Analysis

Uncertainty in the obtained results deals with directly measured and indirectly determined numbers. The directly measured quantities are the following:

- In-cylinder pressure,
- Temperature of the exhaust gases and ambient intake air,
- Air flow rate to the engine,
- Engine speed,
- Exhaust gas compositions including NOx, UHC, and CO.

Instrumentation used in tests for measuring these quantities is shown in Table 5. The in-cylinder pressure is measured as a pressure difference by a piezo-ceramic sensor, which is corrected by absolute pressure offset measured by the sensor MPX 5100AP. The sensor MPX is installed in the intake manifold and the absolute pressure offset is determined at the intake valve closure (IVC). To measure the absolute pressure in the cylinder, it was assumed that the absolute in-cylinder pressure should be similar to the pressure in the intake manifold at the crankshaft position corresponding to IVC.

Table 5. Instrumentation of the measurement system.

Instrument	Range	Uncertainty
	CO: 0.000–10.00%	0.1% (FS)
	UHC: 0–9.999%	12 ppm
Exhaust gas analyzer Bosch BEA 350	CO2: 0.00–18.00%	0.1% (FS)
	O2: 0.00–22.00%	0.1% (FS)
	NO: 0–5000 ppm	25 ppm
Flowmeter CGR-01	0.25–25.00 m^3/h	0.1%
	2–10 pC	$\pm$2%
Charge amplifier Kistler 5018A	10–100 pC	$\pm$0.6%
	100–2,200,000 pC	$\pm$0.3%
Pressure sensor: Kistler 6118C	0–200 bar	$\pm$1% (FS)
Pressure sensor: MPX 5100AP	0–1.1 bar	$\pm$2.5% (FS)
Data acq. system: USB-1608HS	$\pm$10 V	16 bits $\pm$1
Thermocouple NiCR-NiAl (K)	(−40)–1140 °C	$\pm$1% (FS)
Encoder PR90	max 6000 rpm	0.3 deg/rev.
Scale and timer for fuel flow rate	80–650 × 10^{-6} kg/s	$\pm$1%

Indirectly determined quantities are as follows: IMEP, indicated efficiency, COV(IMEP), CA0-10, and CA10-90. The IMEP was determined with Equation (1) involving discrete data:

$$IMEP = \frac{1}{V_s} \times \sum_i (p_i \times \Delta V_i),\tag{1}$$

where

ΔV_i—change in cylinder displacement with changing the crank angle from α_i to α_{i+1},
p_i—change in in-cylinder pressure with changing the crank angle from α_i to α_{i+1}.

Indicated efficiency (IE) was calculated with Equation (2):

$$IE = IMEP \times V_s \times n / (120 \times LHV_f \times m_f),\tag{2}$$

where

V_s—cylinder displacement,
n—engine crankshaft speed,
LHV_f—the lower heating value of a fuel,
m_f—fuel flow rate.

The coefficient of variation (COV) of IMEP defined with the following Equation (3) expresses the unrepeatability of consecutive combustion events in a test series.

$$COV(IMEP) = std(IMEP)/mean(IMEP) \times 100\%,\tag{3}$$

where

std(IMEP)—standard deviation from IMEP population of 100 combustion events,
mean(IMEP)—mean of this IMEP population.

Uncertainties for these indirectly measured quantities were determined as the total derivative. However, uncertainty for COV of IMEP was not determined due to its statistical feature.

Heat release rate (HRR, $dQ/d\alpha$) was determined with Equation (4), where differentials were changed to differences.

$$HRR = 1/(\kappa - 1) \times (\kappa \times p \times \Delta V / \Delta\alpha + V \times \Delta p / \Delta\alpha),\tag{4}$$

where κ—specific heat ratio c_p/c_v.

After integrating HRR, the cumulative heat released was obtained and the CA0-10 and CA10-90 were determined from this heat profile for each individual combustion event. Hence, both CA0-10 and CA10-90 were determined as mean values from 100 combustion events. Uncertainty was determined as the standard deviation in this case.

Uncertainties for indirectly determined quantities are given in Table 6.

Table 6. Uncertainty for indirectly measured quantities.

Quantity	Uncertainty	Relative Uncertainty (%)
IMEP	18 kPa	2.2
Indicated efficiency	0.015	3.7
CA0-10	0.55 CA deg	3.5
CA10-90	0.55 CA deg	3.5

3. Results and Discussion

Exemplary in-cylinder pressures from combustion tests of these three fuels are shown in Figure 2. As mentioned earlier, each pressure trace was calculated as the mean trace from a population consisting of 100 consecutive combustion events. As observed, the peak pressures do not differ by more than 2% from each other in the percentage scale. The bigger difference is seen on the pressure rising slope between the ignition point and the location

for the peak pressure. As observed, the plots for n-butanol and Glyc_But are almost the same, unlike the gasoline plot, which features a slower pressure rise between 5 and 13 CA deg, and then remarkably speeds up while the crankshaft rotates in the range from 14 to 16 CA deg aTDC (after top dead center).
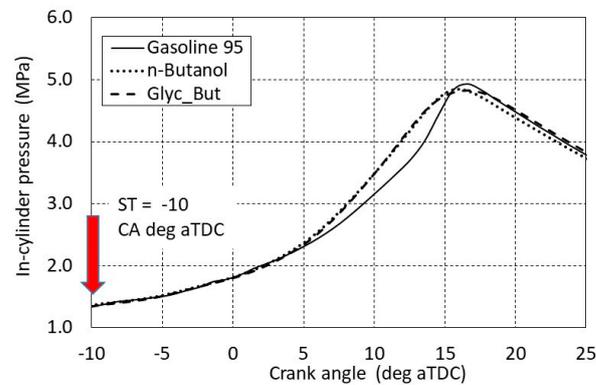

Figure 2. In-cylinder pressure traces vs. crank angle for the tested fuels at fixed spark timing of −10 CA deg aTDC.

3.1. Combustion Thermodynamic Analysis

To investigate more deeply the combustion dynamics, the following quantities were introduced: pressure rise rate, heat release rate, and combustion phases. Figure 3a illustrates pressure rise rate determined as derivative dp/dCA taken from in-cylinder pressure p over the crank angle CA. To provide the same initial conditions for combustion mainly concerning pressure and temperature at the ignition, the spark timing was fixed at −10 CA deg aTDC for these three tested fuels. As depicted, both the n-butanol and the Glyc_But combustion events are characterized with the lower peak of dp/dCA in comparison to the gasoline combustion events. What is more interesting, the addition of glycerol at the amount of 25% to n-butanol does not significantly influence the pressure rise rate and the heat release rate (HRR) (Figure 3b) when compared to the n-butanol test.
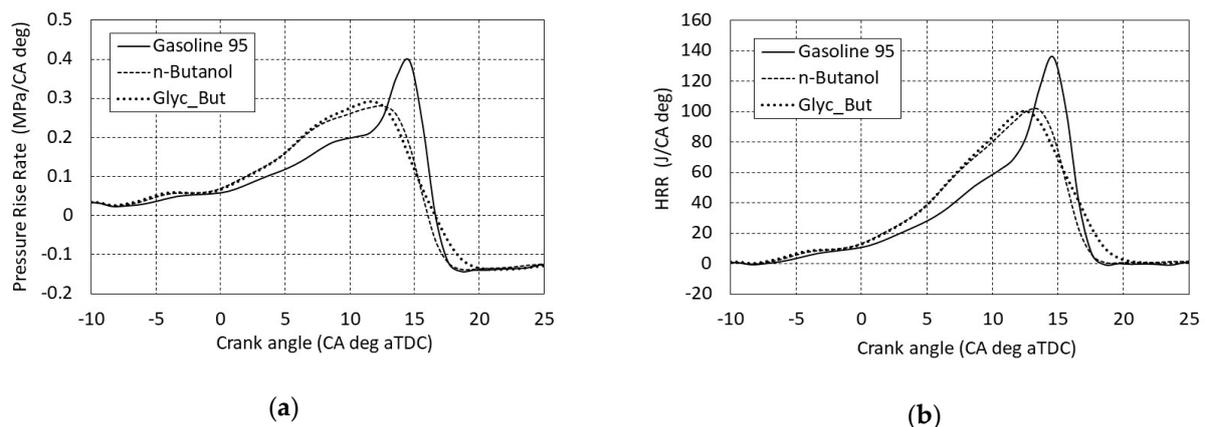

(**a**)

(**b**)

Figure 3. (**a**) Pressure rise rate, (**b**) HRR vs. crank angle for the tested fuels at spark timing of −10 CA deg aTDC.

Based on equations for HRR and its integral denoted as the cumulative heat released, the combustion phases CA0-10 and CA10-90 were determined. As seen in Figure 4a, the longest CA0-10 of 13.3 CA deg is for the gasoline combustion test; the shortest is for n-butanol and equals 12.8 CA deg. Hence, the difference between the shortest and the longest duration of this first CA0-10 phase is not crucial as regards the combustion process at all. The same conclusion can be drawn from Figure 4b, presenting CA10-90. The entire combustion duration expressed as the phase CA0-90 is 25.6, 25.8, and 26.3 CA deg for

gasoline, n-butanol, and Glyc_But, respectively. The relative difference is 2.7% between gasoline and Glyc_But CA0-90 and this is similar to the uncertainty (0.55 CA deg) for the combustion phases. Hence, one can conclude that gasoline and Glyc_But do not differ from each other regarding combustion duration.
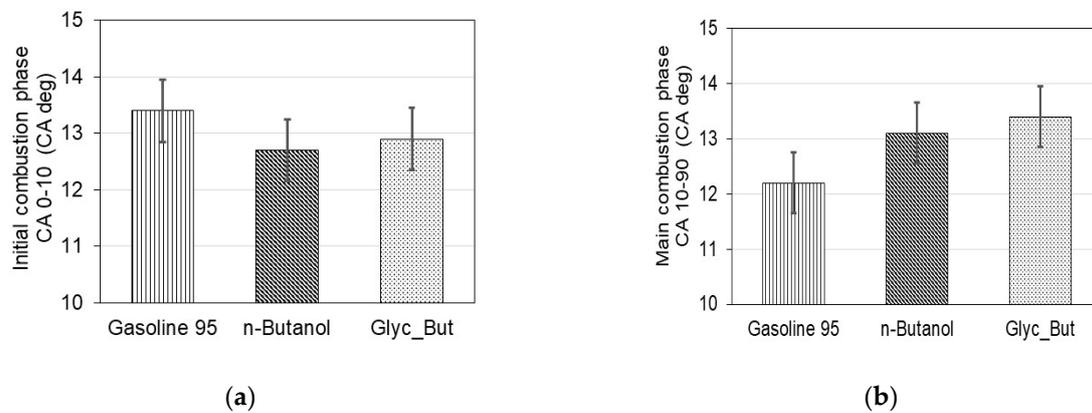

(a)   (b)

Figure 4. Combustion duration phases: (**a**) CA0-10; (**b**) CA10-90 for the tested fuels at fixed spark timing of −10 CA deg aTDC.

3.2. Engine Performance

The engine performance, in this case, is focused on determining the IMEP, indicated efficiency and COV of IMEP. On the basis of the IMEP plot vs. spark timing, the optimal (for maximum IMEP) spark timing can be determined, as depicted in Figure 5. This test was conducted under a constant fuel dose to provide chemical energy in fuel maintained at a similar level for these three fuels.
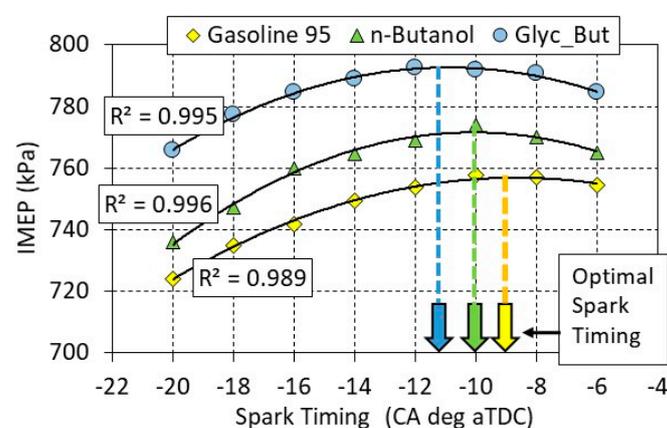

Figure 5. IMEP vs. spark timing for the tested fuels.

As can be seen, the optimal spark timings are −9, −10, and −11 CA deg aTDC and they correspond to IMEPs of 759, 773, and 792 for gasoline 95, n-butanol, and Glyc_But, respectively. A graphical representation of maximum IMEP is shown in Figure 6a. As depicted, IMEP is charged with the uncertainty of 18 kPa, which corresponds to 2.2%. The difference in IMEP for gasoline and Glyc_But is 33 kPa, which stands for 4.3% concerning the IMEP from the gasoline test. This is in the uncertainty limits for IMEP equalling ±2.2%. Taking into account the uncertainty in the fuel flow rate of 1%, one can state that the slight increase in IMEP when replacing gasoline with Glyc_But is confirmed.
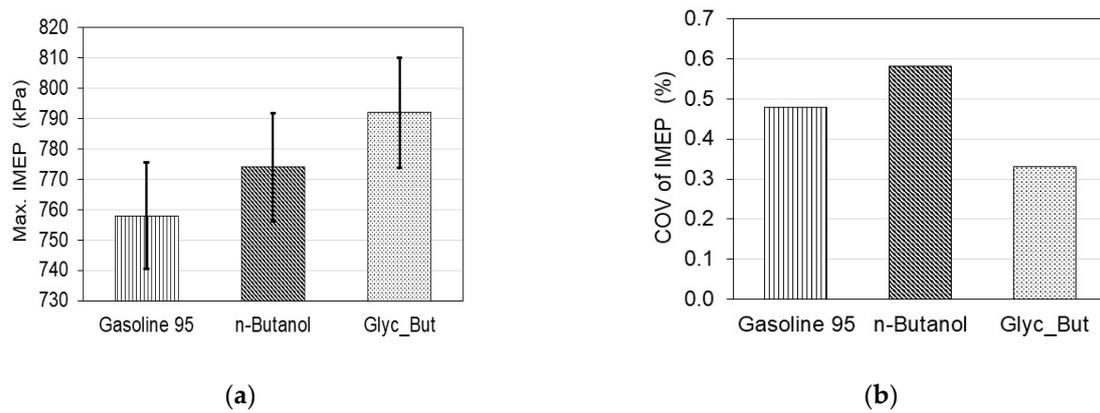
(**a**)

(**b**)

Figure 6. (**a**) Indicated mean effective pressure (IMEP); (**b**) COV of IMEP for the tested fuels at optimal spark timings.

One of the important indicators of engine operation is the COV of IMEP. As mentioned, it expresses the smoothness of engine run. The maximum acceptable limit of the COV of IMEP is 5% for stationary engines working in power generation units. As shown in Figure 6b, the COV of IMEP for all these three tests was significantly below 5%, which indicates good, even excellent, smoothness of engine run.

The last analyzed parameter in this section is the indicated efficiency of the engine, as plotted in Figure 7.
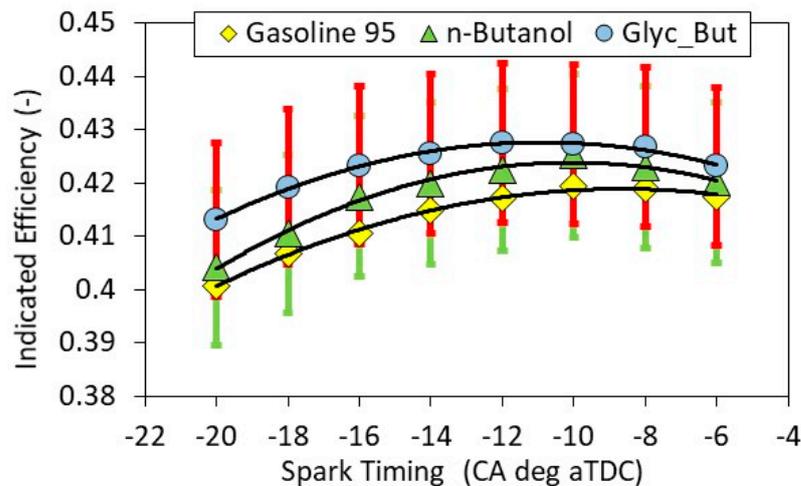
Figure 7. Indicated efficiency vs. spark timing for the tested fuels.

As can be concluded from Figure 7, this efficiency for n-butanol and Glyc_But tests does not deteriorate, and it can even be said that it improves slightly in comparison to the gasoline test. However, one may find that this improvement is questionable because it is within the uncertainty for the indicated efficiency. However, this efficiency improvement can be reasonably explained. During tests, exhaust gas temperature was measured. The exhaust temperature sensor was installed in the tailpipe, approximately 0.5 m away from the engine exhaust valve. Hence, this temperature cannot be considered as the post-flame temperature due to a cooling effect in the tailpipe, but can provide a valuable conclusion. As depicted in Figure 8, the exhaust temperature is the lowest for the engine fueled with the Glyc_But fuel. The decrease is approximately 26 °C. In the Kelvin scale, this temperature drop is approximately 3.4%. Thus, the heat loss in the exhaust gases can decrease in the same ratio, which affects increases in both IMEP and indicated efficiency.
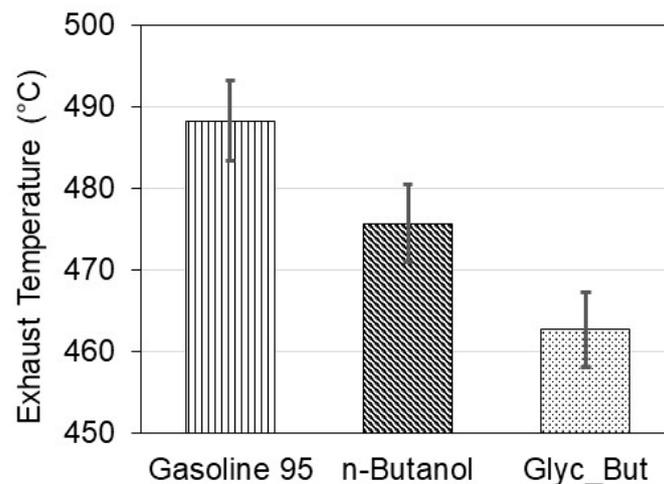
Figure 8. Exhaust gas temperature for the tested fuels at optimal spark timings.

Additionally, the temperature of exhaust gases can reliably express in-cylinder peak and mean combustion temperature, which strongly affects combustion progress, as does combustion rate. Both combustion temperature and exhaust temperature are also affected by the heat of vaporization of both butanol and glycerol content in the blended fuel. As presented in Table 2, the latent heat of vaporization of the Glyc_But fuel is approximately 23% higher than for pure butanol.

3.3. Exhaust Emissions Tests

As depicted in Figure 9a, CO emission was remarkably increased when changing the fuel from either butanol or gasoline to the Glyc_But blend. Relatively short combustion duration, as is typical for IC engines, provides favorable circumstances for increases in CO emissions. Particularly, the high CO emission appears for air–fuel mixtures under a stoichiometric ratio. Hence, the time for the combustion process inside the engine cylinder is not sufficient enough to oxidize CO into CO_2, even though the engine worked at a low speed of 600 rpm. This increase in CO emission is almost two times higher. This was probably caused by the lower combustion temperature, which was indicated by the lower exhaust temperature (Figure 8) in the test with Glyc_But fuel, and it promotes higher emissions of CO. As is well-known, temperature strongly affects chemical reaction rates. Hence, the drop in the exhaust temperature resulting from the in-cylinder combustion temperature affects combustion progress as well as reaction rates for the exhaust toxic compounds NOx, CO, and UHC. UHC (unburnt hydrocarbons) did not increase significantly (Figure 9b) as the CO increased, but UHC emission inversely depends on oxygen bonded in the fuel.

As regards the NOx emission, it depends on the thermal mechanism by Zeldovich [29]. The NOx emission is the lowest for Glyc_But. As concluded from results on the exhaust gas temperatures, the in-cylinder mean combustion temperature is expected to be the lowest for Glyc_But. Thus, NOx formation rate in the flame and post-flame zone for Glyc_But is also the lowest following the Zeldovich thermal NOx mechanism. Thus, lower combustion temperature causes both lower NOx formation and its lower tailpipe emission. As observed in Figure 9b, the NOx emission from Glyc_But combustion strongly decreases by approximately four times as referred to the gasoline test.

Figure 10 shows CO, UHC, and NOx exhaust emissions in energy specific units (g/kWh) for the three fuels tested. As depicted, the trend of NOx confirms the theory that this is correlated with exhaust temperature. Other trends for UHC and CO are also in line with trends presented in Figure 9.
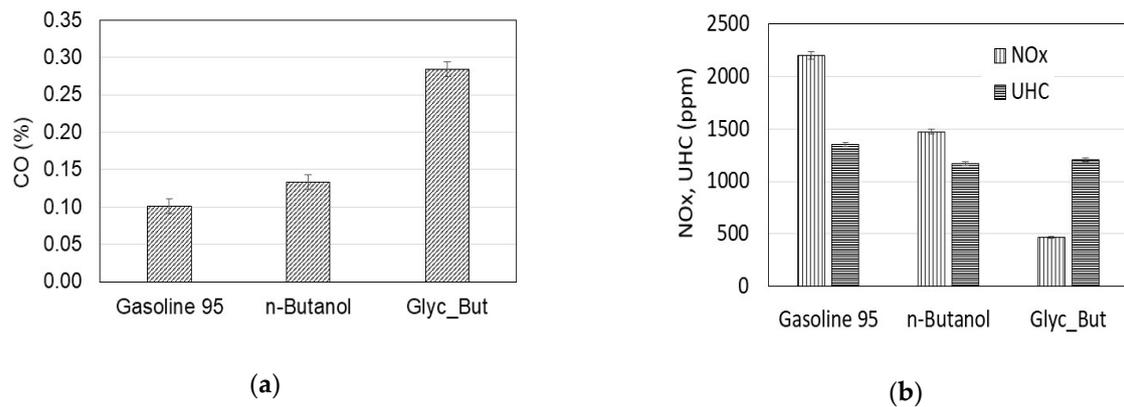
(**a**)

(**b**)

Figure 9. (**a**) CO; (**b**) NOx, and UHC emissions at optimal spark timings for gasoline, butanol, and Glyc_But fuels.
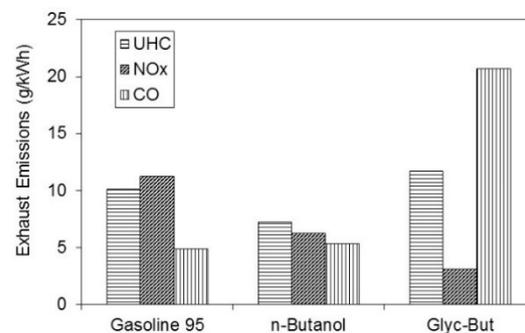

Figure 10. CO; NOx, and UHC specific emissions at optimal spark timings for gasoline, butanol, and Glyc_But fuels.

4. Conclusions

Glycerol, due to its relatively higher viscosity, is difficult to use directly as the fuel for an internal combustion engine. Therefore, blends with alcohols are proposed. This butanol–glycerol blend called Glyc_But is considered a fuel for the spark-ignition internal combustion engine. The following scientific outcomes were confirmed:

- comparative analysis of the fuels tested turned out to be a reliable methodology,
- trends in IMEP, efficiency, and combustion phases were proved,
- NOx emission trend was indirectly affected by the heat of vaporization of a fuel tested (Zeldovich mechanism referring to the exhaust gas temperature).

As observed, glycerol premixed with n-butanol at a ratio of 1:3 (25% glycerol, 75% n-butanol by volume) characterizes similarly to gasoline 95 combustion parameters as follows:

- Engine performance expressed by both the indicated mean effective pressure and the indicated efficiency did not deteriorate. Moreover, these parameters slightly increased, which was caused by lower exhaust gas temperature contributing to the reduction in exhaust heat loss.
- Stability of the engine run was found to be the same for the gasoline 95 test.
- Combustion duration phases CA0-10 and CA10-90 did not differ significantly in comparison to combustion of gasoline 95.
- NOx exhaust emission was reduced by four times in comparison to the test with the gasoline fueled engine. UHC emissions were at a similar level. Unfortunately, CO emissions were twice as high.

Summing up, the proposed glycerol–butanol blend can be applied as a fuel for an internal combustion spark-ignition engine. First of all, this is an effective technology for glycerol utilization. Further investigation in this field is recommended to be continued because glycerol can be considered a fuel for both power generation and means of transport.

References

1. Almena, A.; Bueno, L.; Díez, M.; Martín, M. Integrated biodiesel facilities: Review of glycerol-based production of fuels and chemicals. *Clean Technol. Environ. Policy* **2018**, *20*, 1639–1661. [CrossRef]
2. Emberson, D.R.; Wyndorps, J.; Ahmed, A.; Bjørgen, K.O.P.; Løvås, T. Detailed examination of the combustion of diesel and glycerol emulsions in a compression ignition engine. *Fuel* **2021**, *291*, 120147. [CrossRef]
3. Presciutti, A.; Asdrubali, F.; Baldinelli, G.; Rotili, A.; Malavasi, M.; Di Salvia, G. Energy and Exergy Analysis of Glycerol Combustion in an Innovative Flameless Power Plant. *J. Clean. Prod.* **2018**, *172*, 3817–3824. [CrossRef]
4. Roberts, W.L.; North Carolina State University; Raleigh NC. *Crude Glycerol as Cost-Effective Fuel for Combined Heat and Power to Replace Fossil Fuels, Final Technical Report*; Department of Energy: Washington, DC, USA, 2012.
5. Quispe, C.A.G.; Coronado, C.J.R.; Carvalho, J.A., Jr. Glycerol: Production, Consumption, Prices, Characterization and New Trends in Combustion. *Renew. Sustain. Energy Rev.* **2013**, *27*, 475–493. [CrossRef]
6. Gupta, M.; Kumar, N. Scope and Opportunities of Using Glycerol as an Energy Source. *Renew. Sustain. Energy Rev.* **2012**, *16*, 4551–4556. [CrossRef]
7. Ferreira, A.G.M.; Egas, A.P.V.; Fonseca, I.M.A.; Costa, A.C.; Abreu, D.C.; Lobo, L.Q. The Viscosity of Glycerol. *J. Chem. Thermodyn.* **2017**, *113*, 162–182. [CrossRef]
8. Sliwinski, K.; Marek, W. The Use of Glycerine as Motor Fuel. *Combust. Engines* **2019**, *178*, 166–172. [CrossRef]
9. Bohon, M.D.; Metzger, B.A.; Linak, W.P.; King, C.J.; Roberts, W.L. Glycerol Combustion and Emissions. *Proc. Combust. Inst.* **2011**, *33*, 2717–2724. [CrossRef]
10. Coronado, C.R.; Carvalho, J.A.; Quispe, C.A.; Sotomonte, C.R. Ecological Efficiency in Glycerol Combustion. *Appl. Therm. Eng.* **2014**, *63*, 97–104. [CrossRef]
11. Queirós, P.; Costa, M.; Carvalho, R.H. Co-Combustion of Crude Glycerin with Natural Gas and Hydrogen. *Proc. Combust. Inst.* **2013**, *34*, 2759–2767. [CrossRef]
12. Zhu, M.; Zhang, Z.; Zhang, Y.; Setyawan, H.; Liu, P.; Zhang, D. An Experimental Study of the Ignition and Combustion Characteristics of Single Droplets of Biochar-Glycerol-Water Slurry Fuels. *Proc. Combust. Inst.* **2017**, *36*, 2475–2482. [CrossRef]
13. Beatrice, C.; Di Blasio, G.; Guido, C.; Cannilla, C.; Bonura, G.; Frusteri, F. Mixture of Glycerol Ethers as Diesel Bio-Derivable Oxy-Fuel: Impact on Combustion and Emissions of an Automotive Engine Combustion System. *Appl. Energy* **2014**, *132*, 236–247. [CrossRef]
14. Rodrigues, A.; Bordado, J.C.; Santos, R.G.d. Upgrading the Glycerol from Biodiesel Production as a Source of Energy Carriers and Chemicals—A Technological Review for Three Chemical Pathways. *Energies* **2017**, *10*, 1817. [CrossRef]
15. Grab-Rogalinski, K.; Szwaja, S. The Combustion Properties Analysis of Various Liquid Fuels Based on Crude Oil and Renewables. *IOP Conf. Ser. Mater. Sci. Eng.* **2016**, *148*. [CrossRef]
16. Oprescu, E.-E.; Dragomir, R.E.; Radu, E.; Radu, A.; Velea, S.; Bolocan, I.; Stepan, E.; Rosca, P. Performance and Emission Characteristics of Diesel Engine Powered with Diesel–Glycerol Derivatives Blends. *Fuel Process. Technol.* **2014**, *126*, 460–468. [CrossRef]
17. Eaton, S.J.; Harakas, G.N.; Kimball, R.W.; Smith, J.A.; Pilot, K.A.; Kuflik, M.T.; Bullard, J.M. Formulation and Combustion of Glycerol–Diesel Fuel Emulsions. *Energy Fuels* **2014**, *28*, 3940–3947. [CrossRef]
18. Gruca, M.; Pyrc, M.; Szwaja, M.; Szwaja, S. Effective Combustion of Glycerol in a Compression Ignition Engine Equipped with Double Direct Fuel Injection. *Energies* **2020**, *13*, 6349. [CrossRef]
19. Chwist, M.; Pyrc, M.; Gruca, M.; Szwaja, M. By-Products from Thermal Processing of Rubber Waste as Fuel for the Internal Combustion Piston Engine. *Combust. Engines* **2020**, *181*, 11–18. [CrossRef]
20. Merola, S.; Irimescu, A.; Vaglieco, B. Effect of Fuel Injection Strategy on the Carbonaceous Structure Formation and Nanoparticle Emission in a DISI Engine Fuelled with Butanol. *Energies* **2017**, *10*, 832. [CrossRef]
21. Papagiannakis, R.; Rakopoulos, D.; Rakopoulos, C. Theoretical Study of the Effects of Spark Timing on the Performance and Emissions of a Light-Duty Spark Ignited Engine Running under Either Gasoline or Ethanol or Butanol Fuel Operating Modes. *Energies* **2017**, *10*, 1198. [CrossRef]
22. Lapuerta, M.; González-García, I.; Céspedes, I.; Estévez, C.; Bayarri, N. Improvement of Cold Flow Properties of a New Biofuel Derived from Glycerol. *Fuel* **2019**, *242*, 794–803. [CrossRef]

23. Munsin, R.; Laoonual, Y.; Jugjai, S.; Matsuki, M.; Kosaka, H. Effect of Glycerol Ethoxylate as an Ignition Improver on Injection and Combustion Characteristics of Hydrous Ethanol under CI Engine Condition. *Energy Convers. Manag.* **2015**, *98*, 282–289. [CrossRef]

24. Stelmasiak, Z.; Pietras, D. Utilization of Waste Glycerin to Fuelling of Spark Ignition Engines. *IOP Conf. Ser. Mater. Sci. Eng.* **2016**, *148*. [CrossRef]

25. Fan, Y.; Cai, Y.; Li, X.; Jiao, L.; Xia, J.; Deng, X. Effects of the Cellulose, Xylan and Lignin Constituents on Biomass Pyrolysis Characteristics and Bio-Oil Composition Using the Simplex Lattice Mixture Design Method. *Energy Convers. Manag.* **2017**, *138*, 106–118. [CrossRef]

26. Badrawada, I.G.G.; Susastriawan, A.A.P. Influence of Ethanol-Gasoline Blend on Performance and Emission of Four-Stroke Spark Ignition Motorcycle. *Clean Technol. Environ. Policy* **2019**, *21*, 1891–1896. [CrossRef]

27. Larsson, T.; Mahendar, S.K.; Christiansen-Erlandsson, A.; Olofsson, U. The Effect of Pure Oxygenated Biofuels on Efficiency and Emissions in a Gasoline Optimised DISI Engine. *Energies* **2021**, *14*, 3908. [CrossRef]

28. EU: Fuels: Diesel and Gasoline | Transport Policy. Available online: https://www.transportpolicy.net/standard/eu-fuels-diesel-and-gasoline/ (accessed on 3 August 2021).

29. Zeldovich, Y.B. The oxidation of nitrogen in combustion explosions. *Acta Phys. Ussr* **1946**, *21*, 577–628.